Research Article

Experimental investigations on SS 304 alloy using plasma arc machining

Pothur Hema[1] · Ramprasad Ganesan[1]

Abstract

Plasma arc machining is a well-recognized unconventional machining process widely used to machine intricate part profiles for alloys which are difficult to machine. The surface roughness, material removal rate (MRR), and kerf ratio are predominant factors which influence the performance and quality of plasma cut surfaces. The present research focusses on the effect of plasma arc cutting parameters such as arc voltage, cutting speed, standoff distance, and plasma offset on the cut quality characteristics of SS 304 alloy machined using two different types of nozzles (130 A and 200 A). The experiments were conducted according to a mixed Taguchi design of L18 orthogonal array, and grey relational analysis technique is used for optimization of the above-said cutting conditions. The experimentation on SS 304 alloy is carried out using two different nozzles and identified the best suited nozzle to cut SS 304 alloy of thickness 6 mm which produces better surface roughness and MRR characteristics. Scanning electron microscopy analysis is carried out to inspect the surface morphologies at various cutting conditions.

Keywords Plasma arc cutting · SS 304 alloy · DOE · Optimization · Grey relational analysis

1 Introduction

Among the stainless steel alloys used in the manufacturing industries, SS 304 alloy materials are extensively used in manufacturing of automotive and aerospace structures, in architectural paneling, and even in the marine environment, because of its higher strength and wear resistance. But the machining of the material is difficult by using conventional processes. So among the various unconventional machining processes, one of the most commonly used processes is PAM. It is a thermal energy-based process used for cutting hard materials to a stringent design requirements and complex cutting profiles. The mechanism of material removal in PAM deals with a high-speed gas blown through a constricted nozzle in which some amount of gas is converted into a high-intensity constricted jet of high-temperature plasma arc that is produced between workpiece material and electrode nozzle which is sufficient to raise the workpiece temperature above its melting point that melts/vaporizes the part profile and expels the molten metal away from the cutting region. The PAM process has advantages such as able to cut all electrically conductive materials and to cut high-alloy steel materials with medium and large thicknesses. It is also used in the machining of high-strength structural steel with lower heat input and has a high cutting speed (ten times higher compared to oxy-fuel cutting). In spite of its potential advantages, due to the involvement of several process variables, improving the cut quality characteristics such as MRR and surface roughness is considered to be quite difficult. In order to enhance the cutting quality and performance characteristics of PAM, it is vital to select suitable process variables and their influence in evaluating the

✉ Pothur Hema, hemasvumech@gmail.com; Ramprasad Ganesan, ramprasadofficial16@gmail.com | [1]Department of Mechanical Engineering, S.V. University, Tirupati 517502, India.

part quality. Hence, the plasma arc machining is proposed in this research to analyze the machining of SS 304 alloy.

Maity et al. [1] investigated PAC process by studying a hybrid optimization method on AISI 316 steel, and they found that torch height along with a feed rate is largely contributing to producing an enhanced cutting quality. Subbarao et al. [2] used DOE techniques to investigate the influence of PAC variables on Hardox-400 material, and they proposed that irregularity in cut surface can be reduced by decreasing the cutting speed and other cut quality characteristics depend on arc voltage. Ramakrishnan et al. [3] examined the surface roughness and kerf width during PAC of SS 321 steel by developing regression models and the genetic algorithm was used to to find the optimal solutions. Their result shows that surface roughness and HAZ can be minimum if lower values of current are used, standoff distance, cutting speed, and high gas pressure. Gariboldi et al. [4] identified that by using oxygen as cut gas, the geometrical features of better quality were obtained and they also achieved a better HAZ by using nitrogen, during high-tolerance PAC of titanium sheet. Colombo et al. [5] presented a detailed investigation on plasma arc behavior in the kerf regions during cutting in various operating conditions by high-speed imaging techniques. They also showed that slight imperfections at the nozzle tip caused by erosion can influence the arc symmetry. Cebeli Ozek et al. [6] experimentally predicted the surface roughness in cutting AISI 4140 steel, by developing a fuzzy-based reasoning mechanism. They also showed that the cutting speed has more influence on surface roughness, while the current was minimum. Ananthakumar et al. [7] showed that, with an increase in cutting speed, the kerf taper was affected and regression models for the output parameters were proposed. Bhowmick et al. [8] experimentally studied the PAC of SS 304 grade material and found that an increase in speed and thickness has a significant effect on MRR. Yamaguchi et al. [9] performed a physical investigation on the magnetic arc blow during plasma machining operations and proposed a magnetic shielding cap by experimenting on various nozzles materials. Milan et al. [10] investigated PAC of EN 31 steel and showed that gas pressure has the major influence on the MRR characteristics. Siva Ramakrishna et al. [11] used formulae for the calculation of MRR and validated with adequacy test. Rouniyar et al. [12] performed the experiments and optimized using the grey relational analysis to obtain the optimum parameters on machining the workpiece. Ranganathan et al. [13] used the grey relational analysis for optimizing the machining parameters in hot turning of SS 316 alloy material based on Taguchi technique.

From the literature, it is clear that research of plasma arc machining on SS 304 alloy has received minor importance to researchers but its application is wide in the manufacturing sectors. Moreover, there is a research gap in the selection of suitable nozzle for the machining of the SS 304 alloy material. Hence, this research work focuses on the experimental investigation, analysis and multi-response optimization of the PAM variables to enhance the productivity and quality characteristics on SS 304 alloy material. The following section elaborates the methodologies of the present research work.

2 Methodology

The proposed methodology of this research work involves the selection of material, identification of machine, and determination of process parameters.

2.1 Material selection and machine identification

In this work, SS 304 alloy is selected as the workpiece, which has excellent corrosion and thermal resistance. The chemical composition and physical and mechanical properties of SS 304 alloy are shown in Tables 1 and 2.

Table 2 Physical and mechanical properties of SS 304 alloy

Density	Melting point	Ultimate tensile strength	Elongation	Yield strength
7865 kg/m^3	1400–1415 °C	505 MPa	50%	215 MPa

Fig. 1 CNC plasma arc machine

Table 1 Chemical composition of SS 304 alloy

Cr—18%	Ni—8%	Mn—2%	N—0.10%	S—0.03%
C—0.08%	Si—0.75%	P—0.045%	Remaining Fe	

Table 3 Design variables and levels

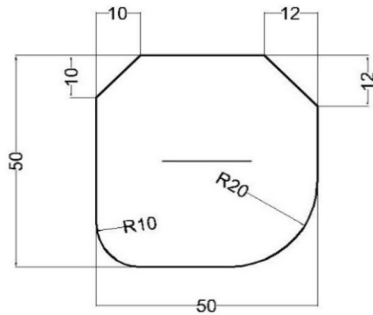| Arc voltage	Cutting speed	Standoff distance	Plasma offset
133 and 136 V	1000, 1500, 2000 mm/min	2, 3.5, 5 mm	1.05, 1.25, 2.25 mm

Fig. 2 Selected profile

Machining of SS 304 alloy was conducted using a high-precision CNC plasma arc machine shown in Fig. 1.

2.2 Selection of process parameters

For conducting the experiments on SS 304 alloy, it has been decided to follow an appropriate orthogonal array design based on the design variables listed in Table 3. The orthogonal array is selected for four design variables, namely arc voltage, cutting speed, standoff distance, and plasma offset. In this study, a mixed Taguchi design L18 (2^1 and 3^3) is selected using Minitab 2017, for each type of nozzle considered.

3 Experimentation

Design of experiments is used to perform the minimum experimentation on the material for each nozzle. Therefore, for the two nozzles, a total of 36 experiments were conducted according to the L 18 orthogonal array design. The machining of the SS 304 alloy material is done by fixing the workpiece on the worktable of the plasma arc machine permanently. The dimension of the workpiece was 817 × 210 mm and thickness of it 6 mm. The present research work identified the profile selection based upon the ability of the plasma torch to cut linear, angular, and curvilinear profiles. The selected profile is shown in Fig. 2. In accordance with the manufacturer's instruction, a number of exhaustive trial experiments were conducted, and finally for the experimentation, two types of nozzles were selected, i.e., 130 A and 200 A, as shown in Fig. 3.
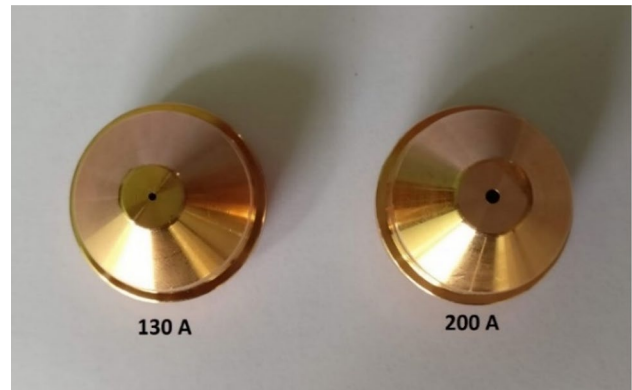

Fig. 3 Nozzle 1 (130 A) and nozzle 2 (200 A)

Fig. 4 Surface roughness tester (side view)

The responses are calculated through two ways, i.e., a) online mode and b) offline mode. During machining, machining time is calculated through online mode. After machining, other responses such as surface roughness are measured by surface roughness tester (Fig. 4), and both top and bottom kerfs are measured by a profile projector (Fig. 5) to calculate kerf ratio. Table 4 gives details about the factors and responses (input and output process parameters) after machining of SS 304 alloy using the two nozzles, respectively, as shown in Fig. 6. In this experimentation, MRR is calculated using the formula with respect to kerf width, cutting length, cutting thickness, and machining time as shown in Eqs. (1, 2). As the SS 304 alloy material is fixed on the worktable of plasma arc machine, the MRR is calculated by using a formula based on the cutting length, thickness of the workpiece and kerf width as shown in the following formulae:

$$\text{Volume} = \left(\frac{\text{Top ker } f + \text{Bottom ker } f}{2} \right) * W/p \text{ thickness} * \text{cutting length} \tag{1}$$

Fig. 5 Profile projector

$$MRR = \frac{Volume * density}{Machining\ time}. \tag{2}$$

4 Results and discussion

In this section, experimental results obtained from the orthogonal array design are discussed. The scheme of experiments to examine the effect of PAM process parameters on performance measures such as surface roughness, kerf ratio, and MRR is optimized in this study, and this is a multi-response optimization problem. For this grey relational analysis, an optimization technique is employed.

4.1 Grey relational analysis

Grey relational analysis [12] is applied to find out the best combination of process parameters for the PAM process. The following formulas given by equations are applied to find the normalization, grey relational coefficient, and grey relational grades. Normalization of original sequence for "larger the better" as in case of MRR is calculated by applying Eq. (3).

$$Z_i^*(k) = \frac{\left[Z_i^*(k) - \min\left\{Z_i^0(k)\right\}\right]}{\left[\max\left\{Z_i^0(k)\right\} - \min\left\{Z_i^k(k)\right\}\right]} \tag{3}$$

where $Z_i^0(k)$ is the original data value obtained from the experimental results, $Z_i^*(k)$ is the normalized value of the experimental results, and in the denominator, max $\{Z_i^0(k)\}$

Table 4 Factors and responses using nozzle 1 (130 A) and nozzle 2 (200 A)

| Sl. no.	Arc voltage (V)	Cutting speed (mm/min)	Standoff distance (mm)	Plasma offset (mm)	Nozzle 1 [130 A]			Nozzle 2 [200 A]		
					Surface roughness (mm)	Kerf ratio	MRR (g/s)	Surface roughness (mm)	Kerf ratio	MRR (g/s)
1	133	1000	2	1.05	1.30	0.60	1.63	1.87	0.60	1.72
2	133	1000	3.5	1.25	1.45	0.55	1.59	2.82	0.55	1.62
3	133	1000	5	2.25	1.78	0.54	1.98	1.61	0.56	1.81
4	133	1500	2	1.05	1.28	0.54	2.95	1.85	0.52	2.92
5	133	1500	3.5	1.25	1.52	0.65	2.78	1.70	0.48	2.92
6	133	1500	5	2.25	1.42	0.66	2.79	1.60	0.52	2.33
7	133	2000	2	1.25	1.62	0.57	3.36	1.38	0.50	3.05
8	133	2000	3.5	2.25	1.79	0.60	2.91	1.66	0.52	3.10
9	133	2000	5	1.05	1.71	0.62	2.93	2.04	0.48	2.59
10	136	1000	2	1.25	2.01	0.61	2.49	1.88	0.56	1.80
11	136	1000	3.5	2.25	1.59	0.55	2.07	1.34	0.57	1.78
12	136	1000	5	1.05	1.59	0.63	1.93	1.30	0.63	2.10
13	136	1500	2	2.25	1.49	0.62	2.98	1.75	0.52	2.63
14	136	1500	3.5	1.05	1.77	0.53	2.73	2.09	0.53	2.22
15	136	1500	5	1.25	1.58	0.57	2.66	1.49	0.52	2.45
16	136	2000	2	2.25	1.16	0.51	3.42	1.78	0.48	3.07
17	136	2000	3.5	1.05	1.31	0.60	3.19	1.68	0.51	3.27
18	136	2000	5	1.25	1.62	0.57	2.87	2.12	0.53	2.77
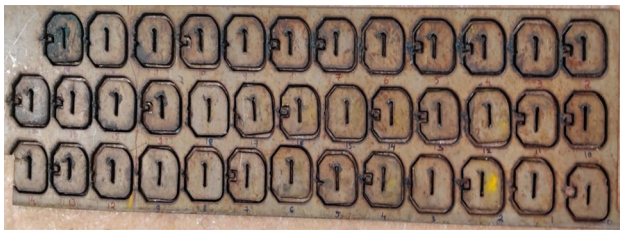
Fig. 6 After machining of SS 304 alloy

is the largest value of $Z_i^0(k)$ and min $\{Z_i^0(k)\}$ implies the smallest value of $Z_i^0(k)$.

Normalization of original sequence for "smaller the better" as in case of kerf ratio and surface roughness is calculated by applying Eq. (4).

$$Z_i^*(k) = \frac{\left[\max\{Z_i^0(k)\} - Z_i^*(k)\right]}{\left[\max\{Z_i^0(k)\} - \min\{Z_i^k(k)\}\right]}. \tag{4}$$

The grey relational coefficient (GRC) is calculated using Eq. (5).

$$GRC = \frac{\left[\Delta_{min} + \alpha\Delta_{max}\right]}{\left[\Delta_{oi}^* + \alpha\Delta_{max}\right]} \tag{5}$$

where α = distinguishing coefficient. Generally, the value of $\alpha = 0.5$ is used. $0 < GRC < 1$

Deviation is calculated by using Eq. (6).

$$\Delta_{oi}^* = \frac{1}{n}\sum_{k=1}^{n}\Delta_{oi}(k) \tag{6}$$

where $\Delta_{0i}(k)$ is the deviation sequence of the reference sequence $x_0^*(k)$.

After calculating the grey relational coefficient of the performance parameters, the average value of the grey relational coefficient is calculated as the grey relational grade (GRG). Using Eq. (7), the grey relational grade is calculated.

$$GRG = \frac{1}{n}\sum_{k=1}^{n}GRC(k). \tag{7}$$

In Table 5, the grey relational coefficient and grey relational grade are calculated for both nozzles.

Basically, the experimental number which achieves the maximum GRG value is considered as the ideal experiment to obtain an improved product quality. Hence, out of the 18 experiments performed, the maximum grey relational grade is achieved for 16th experiment and the optimized machining parameter for machining the

Table 5 Results of grey relational analysis for SS 304 alloy using nozzle 1 (130 A) and nozzle 2 (200 A)

Nozzle 1 (130 A) Exp. no	Grey relation coefficient			GRG	Nozzle 2 (200 A) Exp. no	Grey relation coefficient			GRG
	Kerf Ratio	SR	MRR			Kerf ratio	SR	MRR	
1	0.463	0.756	0.338	0.519	1	0.391	0.573	0.347	0.437
2	0.675	0.593	0.333	0.534	2	0.522	0.333	0.333	0.396
3	0.698	0.404	0.388	0.497	3	0.481	0.711	0.362	0.518
4	0.728	0.779	0.659	0.722	4	0.662	0.579	0.702	0.648
5	0.342	0.543	0.588	0.491	5	0.951	0.658	0.705	0.771
6	0.333	0.620	0.590	0.514	6	0.640	0.720	0.469	0.610
7	0.551	0.481	0.933	0.655	**7**	**0.778**	**0.905**	**0.796**	**0.826**
8	0.444	0.401	0.640	0.495	8	0.665	0.677	0.835	0.726
9	0.407	0.436	0.650	0.498	9	1.000	0.507	0.551	0.686
10	0.420	0.333	0.495	0.416	10	0.479	0.566	0.359	0.468
11	0.661	0.498	0.404	0.521	11	0.466	0.946	0.357	0.590
12	0.388	0.496	0.379	0.421	12	0.333	1.000	0.414	0.582
13	0.408	0.564	0.674	0.549	13	0.643	0.629	0.565	0.612
14	0.840	0.410	0.570	0.607	14	0.582	0.491	0.441	0.505
15	0.556	0.500	0.547	0.534	15	0.674	0.803	0.503	0.660
16	**1.000**	**1.000**	**1.000**	**1.000**	16	0.991	0.613	0.804	0.803
17	0.453	0.738	0.795	0.662	17	0.707	0.669	1.000	0.792
18	0.542	0.481	0.624	0.549	18	0.599	0.483	0.626	0.569

Table 6 Response table for GRG for nozzle 1

Response table for GRG				
Level	Arc voltage	Speed	SOD	Plasma offset
1	0.5472	0.4847	0.6434	0.576
2	0.5844	0.5695	0.5516	0.5331
3	–	0.6432	0.5023	0.5882
Delta	0.0372	0.1585	0.1412	0.055
Rank	4	1	2	3

Table 7 Response table for GRG for nozzle 2

Response table for GRG				
Level	Arc voltage	Speed	SOD	Plasma offset
1	0.5472	0.4847	0.6434	0.576
2	0.5844	0.5695	0.5516	0.5331
3	–	0.6432	0.5023	0.5882
Delta	0.0372	0.1585	0.1412	0.055
Rank	4	1	2	3

Fig. 8 Cutting speed versus GRG

Fig. 9 Standoff distance versus GRG

Fig. 7 Arc voltage versus GRG

SS 304 alloy using nozzle 1 (130 A) is obtained, and for second set of experiments using nozzle 2 (200 A), the seventh experiment has the highest GRG value. Tables 6 and 7 show the response table for GRG and specify the rank of the input parameters which has the most influence on machining the material.
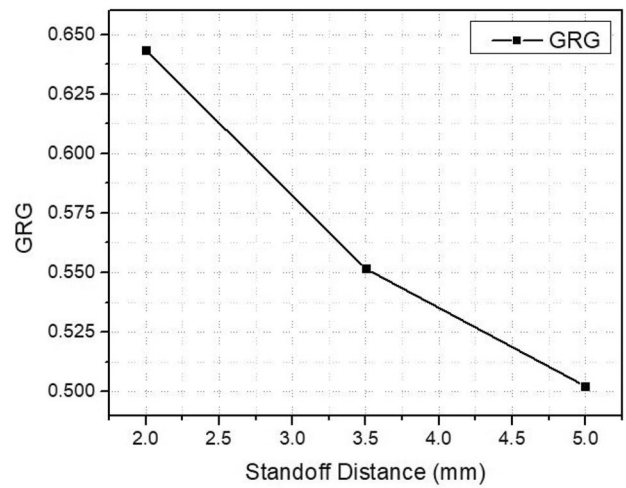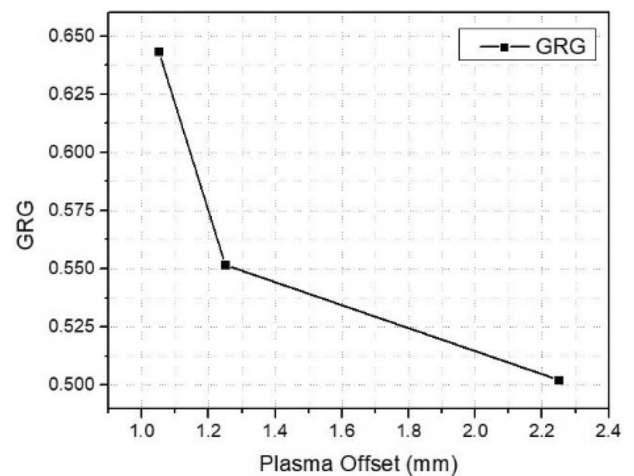
Fig. 10 Plasma offset versus GRG
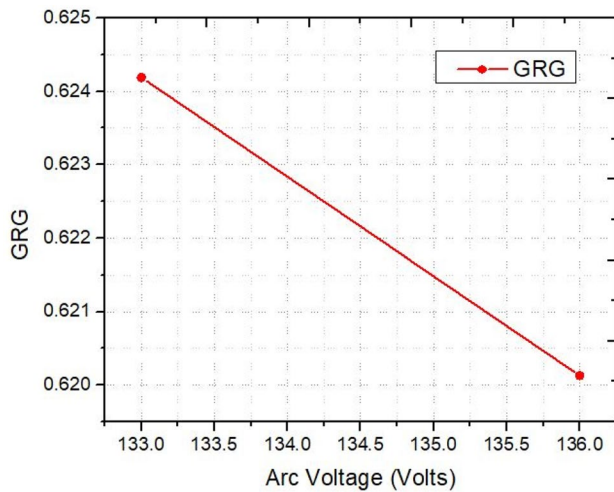
Fig. 11 Arc voltage versus GRG
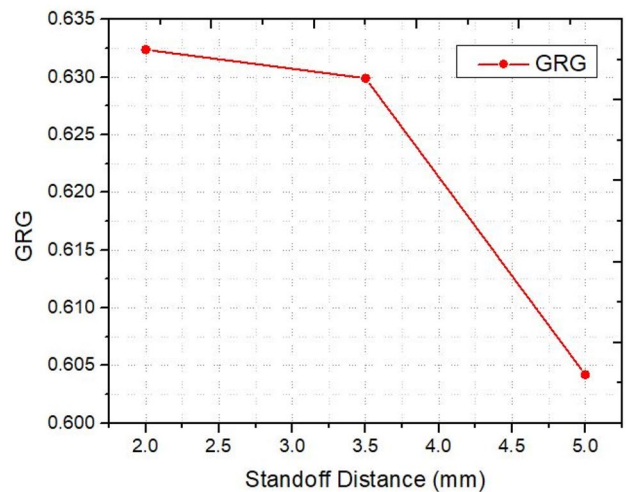
Fig. 13 Standoff distance versus GRG
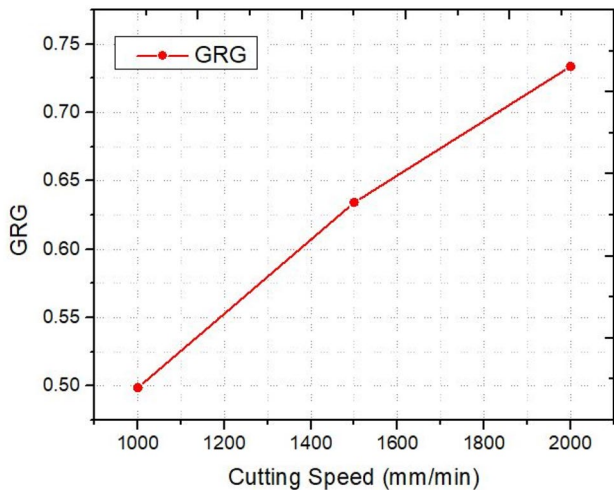
Fig. 12 Cutting speed versus GRG
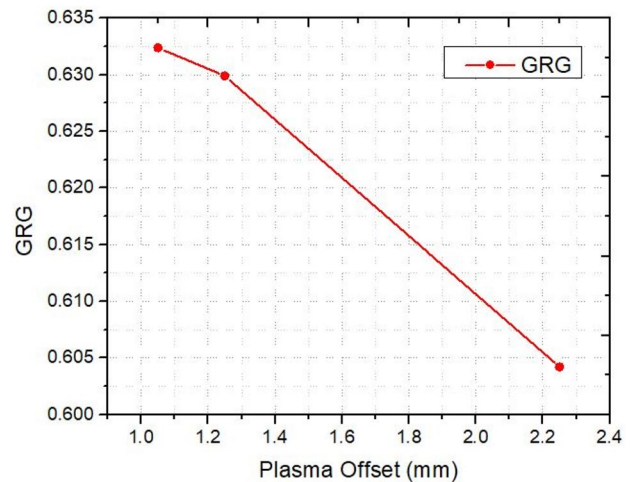
Fig. 14 Plasma offset versus GRG

4.2 GRG versus inputs

The GRG is the normalized output of all the output parameters such as kerf ratio, surface roughness, and MRR. The highest GRG point represents the most optimum input parameters that can be used for obtaining minimum kerf ratio, surface roughness, and maximum MRR, respectively, as shown in Figs. 7, 8, 9, 10, 11, 12, 13, and 14.

4.3 Selection of best nozzle for cutting SS 304 alloy

Before performing the validation test, the best nozzle must be selected which gives higher MRR and lesser SR and kerf ratio. In the following sections, the best nozzle suited for

machining SS 304 alloy is chosen by carefully examining the performance graphs and by the SEM analyses. The performance of each output parameter with respect to each input process parameter is examined using performance graphs which are discussed in the following.

(a)   Kerf ratio versus inputs

The kerf ratio should be maintained as low as possible, and it is compared for the two nozzles, as shown in Figs. 15, 16, 17, and 18. From the grey relational analysis, it is seen that arc voltage has the least influence on the kerf ratio, and from Fig. 15, it is observed that when the material is machined using 130 A nozzle, the kerf ratio is decreasing with respect
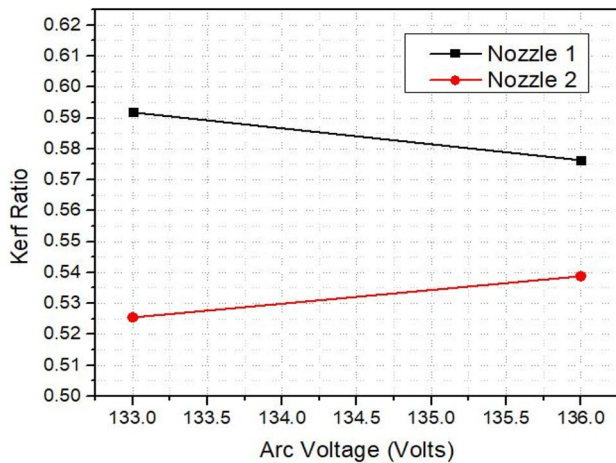
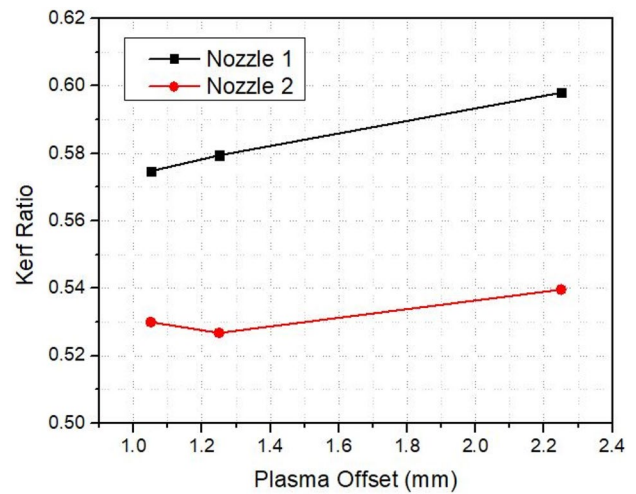Fig. 15 Arc voltage versus kerf ratio
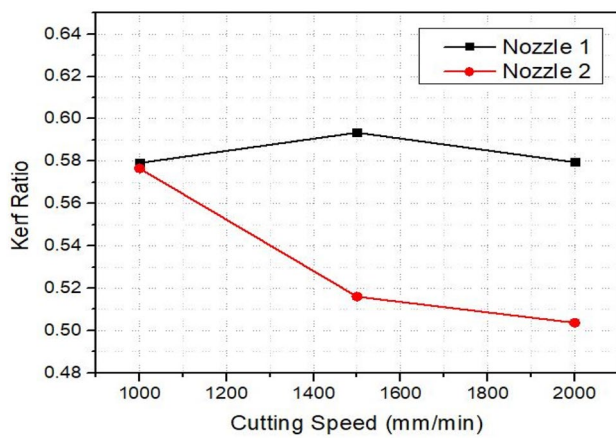

Fig. 18 Plasma offset versus kerf ratio

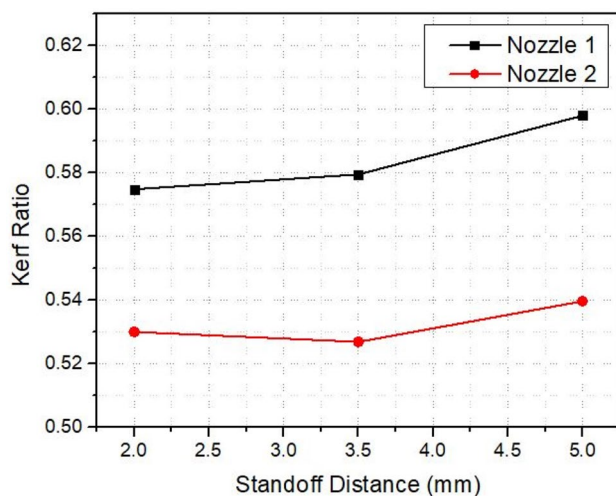Fig. 16 Cutting speed versus kerf ratio

Fig. 17 Standoff distance versus kerf ratio

to an increase in arc voltage, and this is due to the fact that a high-intensity plasma jet is expelled from a smaller-diameter nozzle, resulting in irregular kerfs. But using 200 A nozzle, even though the kerf ratio is increasing with respect to the increase in arc voltage, due to the larger diameter nozzle the plasma arc width is maintained constant, thus enabling accurate kerfs. The influence of cutting speed with respect to the kerf ratio is depicted in Fig. 16. It is observed that in 130 A nozzle, the kerf ratio is slightly increasing and reduces to a minimum value. For 200 A nozzle, the kerf ratio is decreasing drastically till it reaches a minimum value. Here, faster cuts produce finer kerfs due to lesser penetration of the plasma jet on the work piece; hence, better kerf ratio characteristics are produced by the 200 A nozzle having a larger diameter. Figure 17 depicts the influence of standoff distance on the kerf ratio. By using both types of nozzles, the kerf ratio increases with respect to the increase in the standoff distance, since at higher distances there will be a lack of energy input from the plasma arc which leads to narrow kerfs. From Fig. 18, it is observed that the kerf ratio is increasing with respect to an increase in the plasma offset for both the nozzles. The plasma offset is a parameter which maintains the arc width of the plasma; with increasing arc width, higher kerf ratios are obtained.

(b) Surface roughness versus inputs

The surface roughness should be maintained as low as possible, and it is compared for the two nozzles, as shown in Figs. 19, 20, 21, and 22. The influence of arc voltage on surface roughness is depicted in Fig. 19, which demonstrates that by using 130 A nozzle, the surface roughness
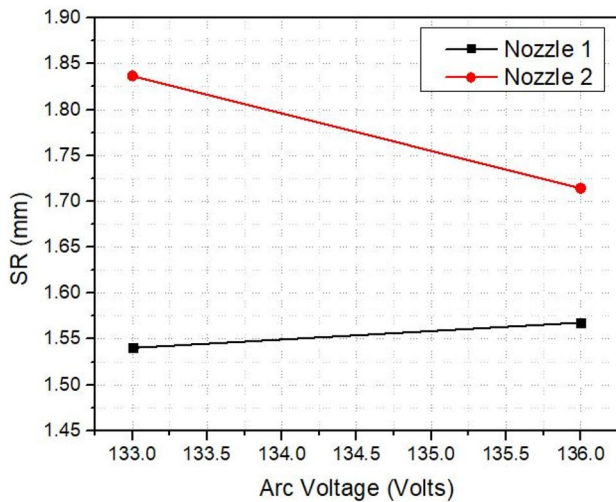
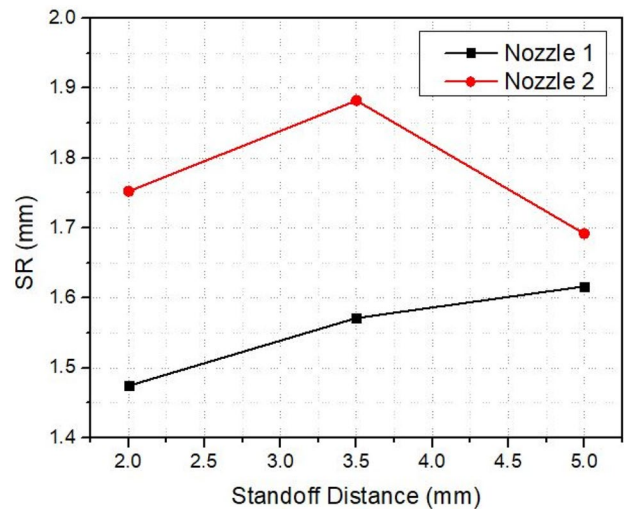**Fig. 19** Arc voltage versus surface roughness

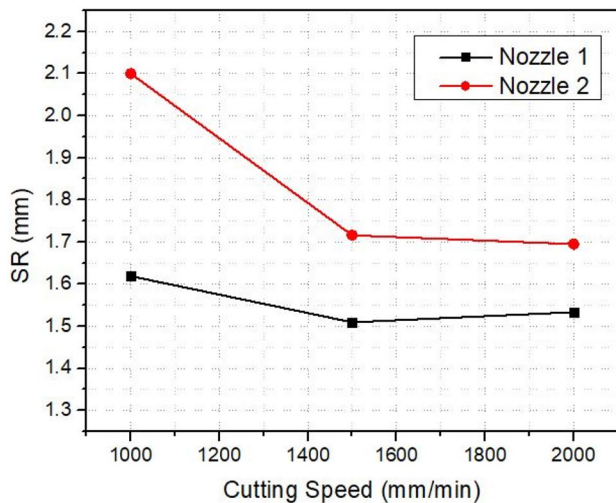**Fig. 21** Standoff distance versus surface roughness

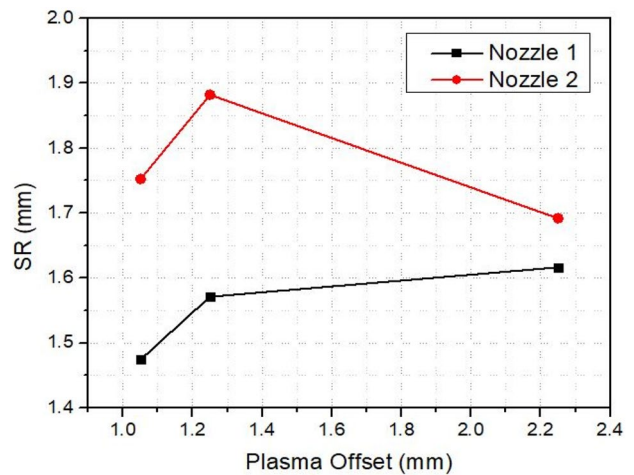**Fig. 20** Cutting speed versus surface roughness

Fig. 22 Plasma offset versus surface roughness

increases with respect to an increase in arc voltage and the least value is obtained. While using 200 A nozzle for cutting, the surface roughness is decreasing with respect to an increase in arc voltage. Generally, a high-intensity plasma arc produces a rough surface finish because of a high exothermic reaction taking place along the cutting region. From Fig. 20, it is observed that with increasing cutting speed, the surface roughness reduces to a minimum value for both the nozzles, and this is due to the fact that an increase in cutting speeds leads to lesser heat

zones along the kerf region, thus producing better surface finish. The influence of standoff distance on surface roughness is shown in Fig. 21. In 130 A nozzle, the surface roughness is minimum at the starting and increases gradually. In 200 A nozzle, the surface roughness is increasing from standoff distance 2 to 3.5 mm and reduces to a minimum value. The best surface finish is obtained at a minimum standoff distance as the molten metal gets vaporized very quickly along the cutting length. From Fig. 22, it is clear that the least surface roughness is achieved with the least
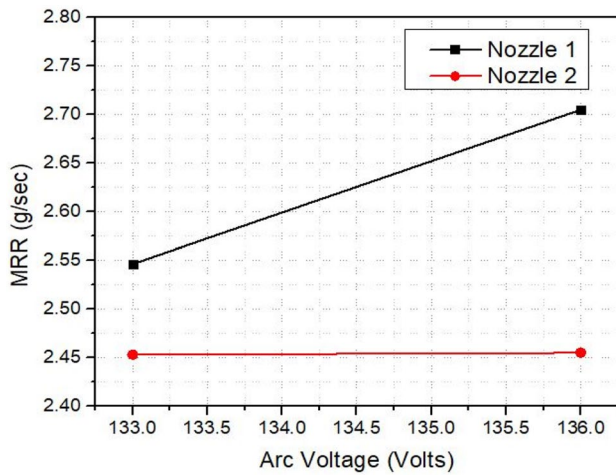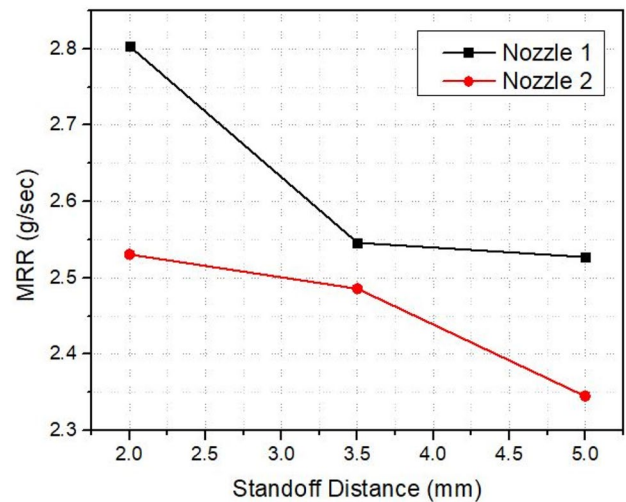
Fig. 23 Arc voltage versus MRR
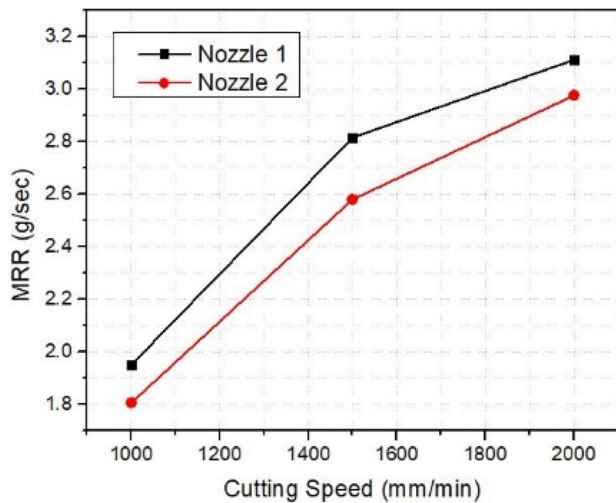

Fig. 25 Standoff distance versus MRR

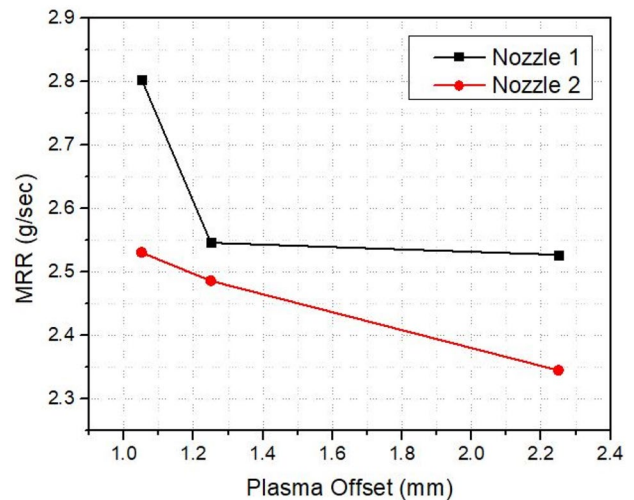**Fig. 24** Cutting speed versus MRR

Fig. 26 Plasma offset versus MRR

plasma offset value as the arc width is maintained minimum. Hence, 130 A nozzle which has a small diameter with the minimum plasma offset produces better surface finish than 200 A nozzle.

(c)   MRR versus inputs

The MRR should be maintained as high as possible, and it is compared for the two nozzles, as shown in Figs. 23,

24, 25, and 26. The arc voltage has the least influence on the cutting speed as it is shown in Fig. 23. There is a slight increase in MRR from 133 volts to 136 volts in both the nozzles. Form Fig. 24, it is observed that the cutting speed has the highest influence on MRR, as an increasing trend is observed in both the nozzles. Here, out of the two nozzles, 130 A nozzle shows a better MRR characteristics than 200 A nozzle. The influence of standoff distance on MRR is depicted in Fig. 25. Here, for both the nozzles, the MRR is drastically decreasing with respect to an increase
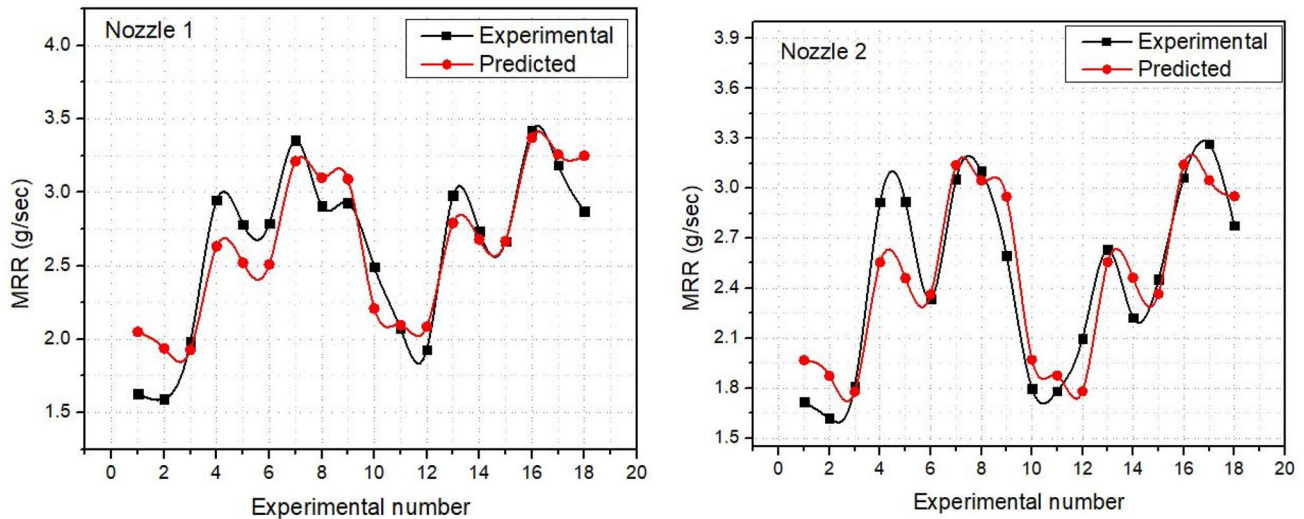
Fig. 27 Comparison between experimental and predicted MRR for nozzle 1 (130 A) and nozzle 2 (200 A)

in standoff distance because higher standoff distance reduces the arc coherence leading to divergence of the plasma arc. From Fig. 26, it is observed that for both the nozzles, a decreasing trend of MRR with an increase in plasma offset is achieved and still 130 A nozzle has higher MRR than the other nozzle.

4.4 Statistical analysis for MRR

A regression analysis is used for calculating MRR for both nozzle 1 (130 A) and nozzle 2 (200 A). Hence, the following linear regression equations (Eqs. 1, 2) are generated using Minitab software. A minimal average error is 20% for MRR. The comparison results show better closeness between the predicted response values and experimental results, as shown in Fig. 27, and hence, the developed approach can be suitable for assessing the cutting characteristics in PAC of SS 304 alloy.

1. For nozzle type 1 (130A)

$$\begin{aligned} \text{MRR (g/sec)} = \{&-6.11 + (0.0530 \times \text{Arc voltage}) \\ &+ (0.001162 \times \text{Cutting speed}) \\ &- (0.0923 \times \text{Standoff distance}) \\ &+ (0.128 \times \text{Plasma offset})\}. \end{aligned} \tag{1}$$

2. For nozzle type 2 [200A]

$$\begin{aligned} \text{MRR (g/sec)} = \{&0.83 + (0.0007 \times \text{Arc voltage}) \\ &+ (0.001172 \times \text{Cutting speed}) \\ &- (0.0621 \times \text{Standoff distance}) \\ &- (0.003 \times \text{Plasma offset})\} \end{aligned} \tag{2}$$

5 Surface morphology

SEM images were taken to inspect the effect of high-temperature plasma gas on the machined surface of SS 304 alloy. From the examination of the surface characteristics of SS 304 alloy machined using the nozzles 1(130 A) and 2 (200 A), it was observed that the process produces spattered drops, pockmarks, globules of debris, and varying size craters on the workpiece surface. The surface produced by nozzle 1 (130 A) has fewer globules of debris, cracks, and craters as shown in Fig. 28. It is observed from Fig. 29 that white layer, melted drops, craters, and cracks are more pronounced, when the material is machined using nozzle 2 (200 A). This also makes the surface rough and having uneven surface profile because nozzle 2 (200 A) has a larger
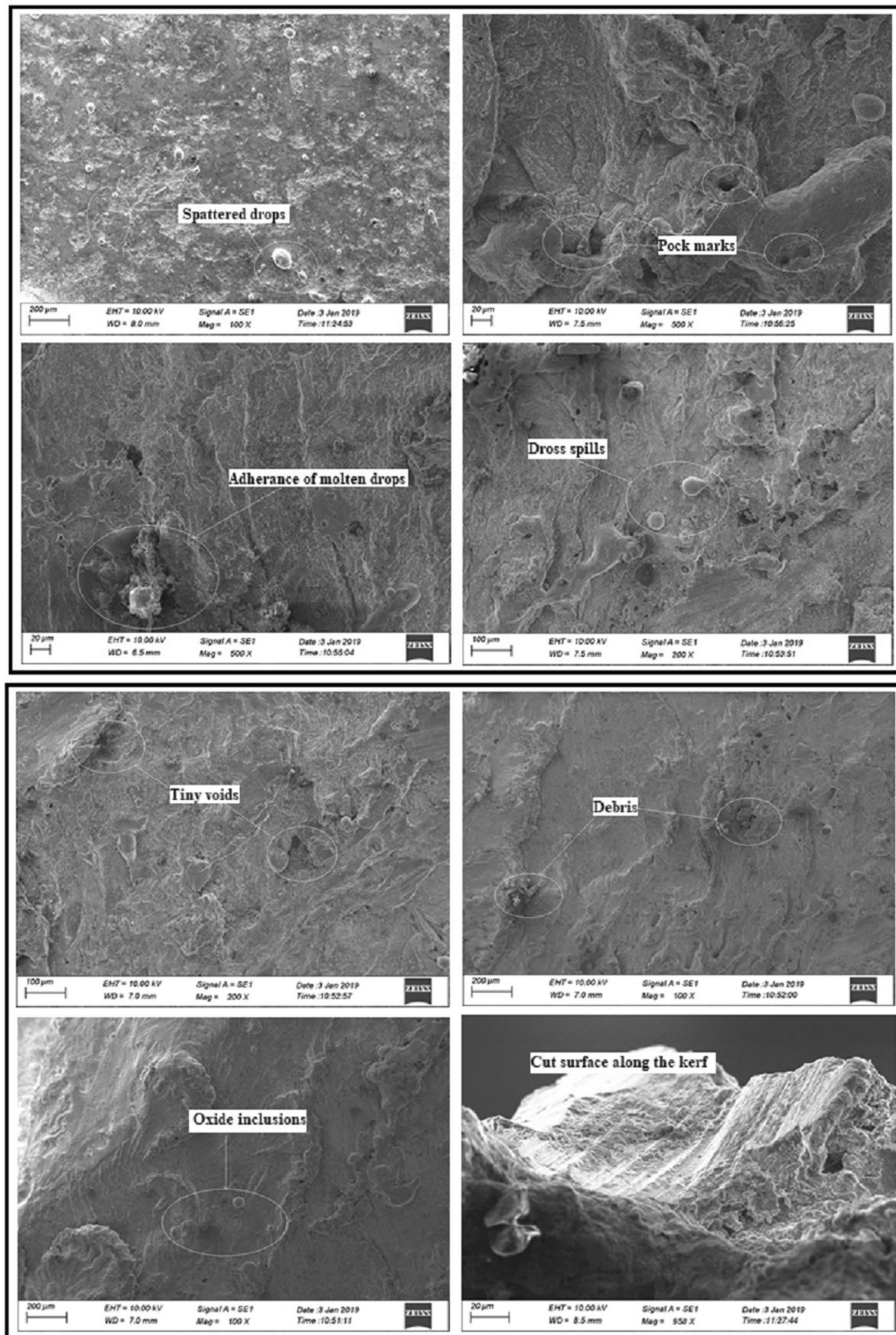
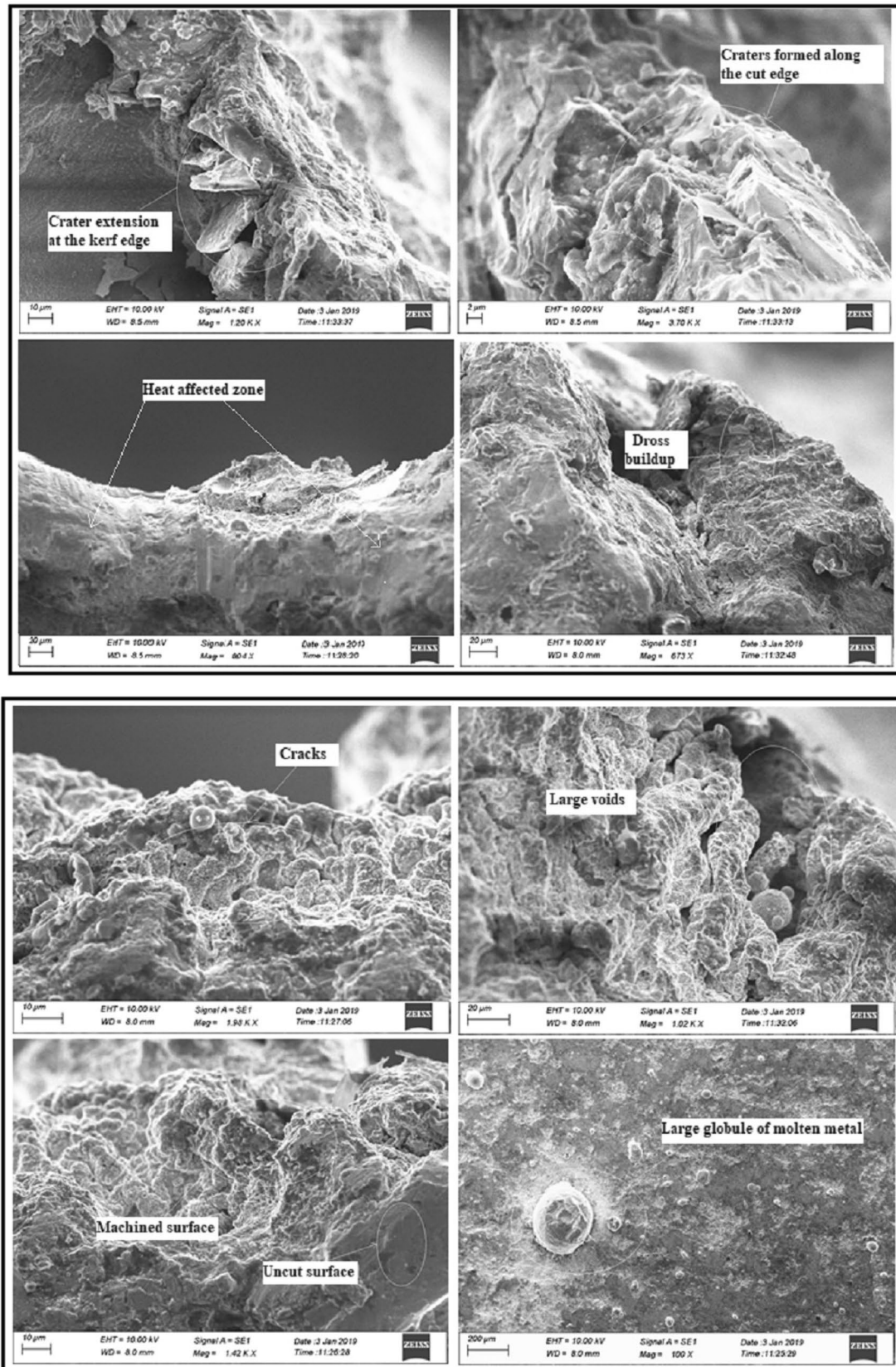**Fig. 28** SEM morphology of SS 304 alloy machined using nozzle 1

Fig. 29 SEM morphology of SS 304 alloy machined using nozzle 2

Table 8 Validation test on SS 304 alloy using nozzle 1

Input parameters				Output parameters		
Arc voltage (V)	Cutting speed (mm/min)	Standoff distance (mm)	Plasma offset (mm)	Kerf ratio	Surface roughness (mm)	MRR (g/s)
136	2000	2	2.25	0.486	1.159	3.79

diameter and helps immediate solidification of molten drops near the top kerf region.

6 Validation test

From the experiments conducted using 130 A nozzle, the grey relational analysis indicates that the 16th level has the maximum GRG value of 1.0, and it is considered as the optimum level out of the levels selected for the experimentation. To confirm this, a validation test was conducted for the 16th level of experiment, and the response values obtained are shown in Table 8, and Fig. 30 represents the results of validated specimen which shows better kerf ratio and minimal surface defects after machining.

7 Conclusions

Based on the careful experimental research of CNC PAM on SS 304 alloy using two different nozzles, the following conclusions are highlighted:

- The experimental results clearly show that an arc voltage of 136 volts, cutting speed of 2000 mm/min, standoff distance of 2 mm, and plasma offset of 2.25 mm will give the optimum results for PAM of SS 304 alloy by implementing multi-response optimization technique using grey relational analysis.
- Based on GRA, the response tables were established for both the nozzles, from which it is concluded that cutting speed and standoff distance have the most influence, while plasma offset and arc voltage have the least influence on the kerf ratio, surface roughness, and MRR in PAM of SS 304 alloy.
- Finally, the best suited nozzle for machining the SS 304 alloy material which yields better surface roughness and MRR characteristics were determined with the aid of performance graphs.
- 200 A Nozzle produces more accurate kerfs due to its larger nozzle diameter and maintains lesser kerf ratio than nozzle 1.
- 130 A Nozzle has a smaller nozzle diameter and can produce higher MRR while maintaining lower surface roughness. Hence, 130 A nozzle is selected as the best suited nozzle for machining SS 304 alloy material.
- The surface morphology was studied carefully on both the materials to understand how the high-temperature plasma gas influences the machined surface and its characteristics during machining.
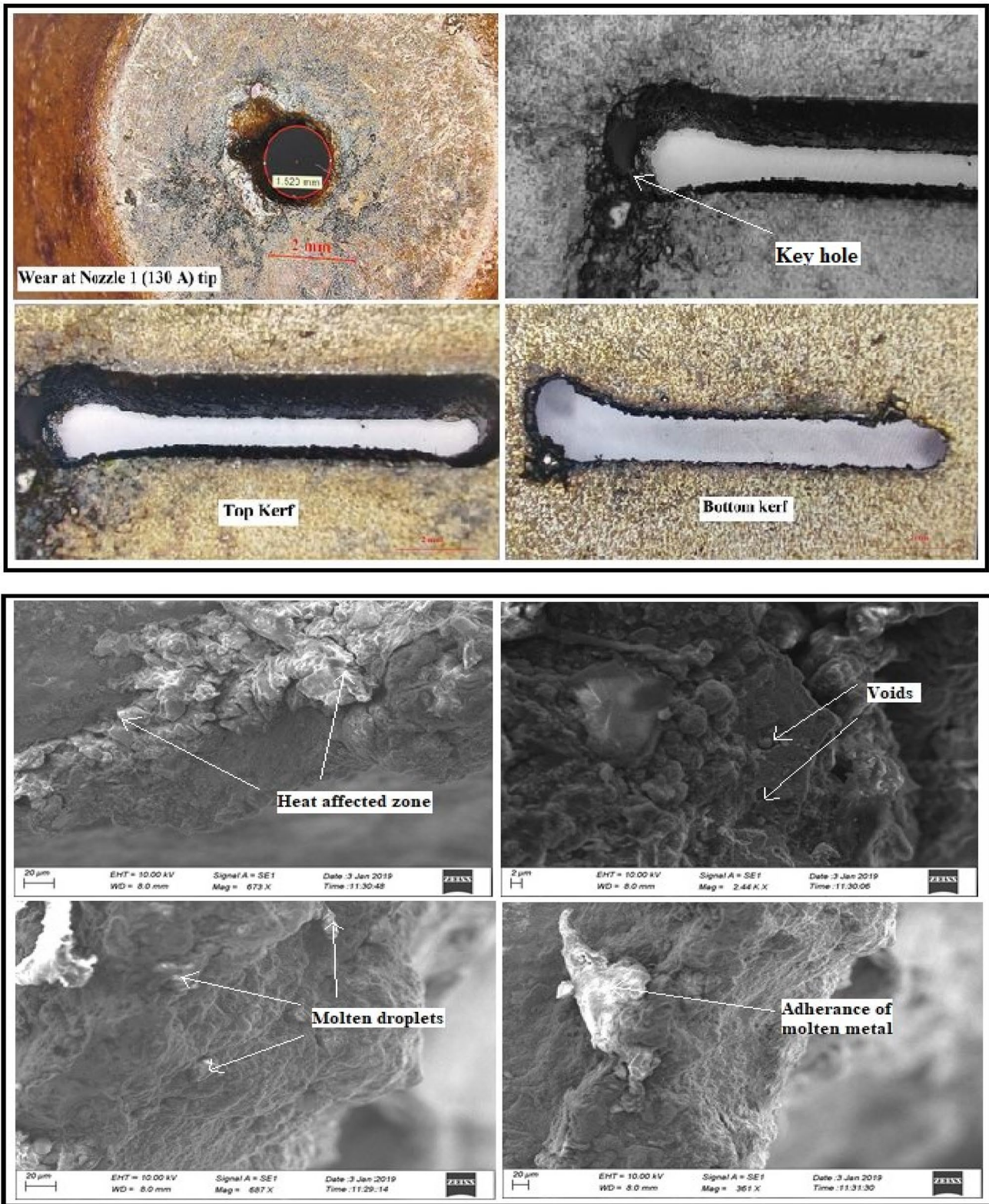
Fig. 30 Nozzle wear and SEM images of validation test results

Compliance with ethical standards

Conflict of interest On behalf of all authors, the corresponding author states that there is no conflict of interest.

References

1. Maity KP, Bagal DK (2015) Effect of process parameters on cut quality of stainless steel of plasma arc cutting using hybrid approach. Int J Adv Manuf Technol 78:161–175
2. Subbarao Chamarthi N, Reddy S, Elipey MK, Ramana Reddy DV (2013) Investigation analysis of plasma arc cutting parameters on the unevenness surface of Hardox-400 material. Proc Eng 64:854–861
3. Ramakrishnan H, Balasundaram R, Ganesh N, Karthikeyan N (2018) Experimental investigation of cut quality characteristics on SS321 using plasma arc cutting. J Braz Soc Mech Sci Eng 40(2):60
4. Gariboldi E, Previtali B (2005) High tolerance plasma arc cutting of commercially pure titanium. J Mater Proces Technol 160(1):77–89. https://doi.org/10.1016/j.jmatprotec.2004.04.366
5. Colombo V, Concetti A, Ghedini E, Dallavalle S, Vancini M (2009) High-speed imaging in plasma arc cutting: a review and new developments. Plasma Sources Sci Technol. https://doi.org/10.1088/0963-0252/18/2/023001
6. Ozek C, Caydas U, Unal E (2012) A fuzzy model for predicting surface roughness in plasma arc cutting of AISI 4140 steel. Mater Manuf Process 27:95–102
7. Ananthakumar K, Rajamani D, Balasubramanian E, Paulo Davim J (2018) Measurement and optimization of multi-response characteristics in plasma arc cutting of Monel 400TM using RSM and TOPSIS. Measurement. https://doi.org/10.1016/j.measurement.2018.12.010
8. Bhowmick S, Basu J, Majumdar G, Bandyopadhyay A (2018) Experimental study of plasma arc cutting of AISI 304 stainless steel. Mater Today Proc 5:4541–4550
9. Yamaguchi Y, Katada Y, Itou T, Uesugi Y, Tanaka Y, Ishijima T (2015) Experimental study of magnetic arc blow for plasma arc cutting. Weld Int 29:745–753
10. Das MK, Kumar K, Barman TK, Sahoo P (2014) Optimization of process parameters in plasma arc cutting of EN 31 steel based on MRR and multiple roughness characteristics using grey relational analysis. Proc Mater Sci 5:1550–1559
11. Siva Ramakrishna Ch, Raghuram KS, Avinash Ben B (2018) Process modelling and simulation analysis of CNC oxy-fuel cutting process on SA 516 grade 70 carbon steel. Mater Today Proc 5:7818–7827
12. Rouniyar AK, Shandilya P (2018) Multi-objective optimization using Taguchi and grey relational analysis on machining of Ti–6Al–4V Alloy by powder mixed EDM process. Mater Today Proc 5(11):23779–23788
13. Ranganathan S, Senthilvelan T (2011) Multi-response optimization of machining parameters in hot turning using grey analysis. Int J Adv Manuf Technol 56(5–8):455–462

Publisher's Note Springer Nature remains neutral with regard to jurisdictional claims in published maps and institutional affiliations.